School of Pharmaceutical Sciences[1], São Paulo State University, Araraquara; Physics Institute of São Carlos[2], University of Sao Paulo; Paulista Central University Center[3], Sao Carlos, Brazil

Curcumin-loaded cationic solid lipid nanoparticles as a potential platform for the treatment of skin disorders

M. L. Gonçalez[1,*], R. B. Rigon[1], M. A. Pereira-da-Silva[2,3], M. Chorilli[1]

Received June 9, 2017, accepted July 28, 2017

**Corresponding author: Maíra Lima Gonçalez, Km 1, Araraquara-Jau Road. Zip code: 14801-902, Sao Jose do Rio Preto, Sao Paulo, Brazil*
goncalez.m.l@gmail.com

Pharmazie 72: 721–727 (2017) *doi: 10.1691/ph.2017.7101*

Curcumin (CUM) possesses therapeutic activity against diverse skin disorders (SD); however, its clinical use faces many challenges related to physicochemical and bioavailability characteristics, that can be solve designing a new drug delivery system for CUM to treat SD. Cationic solid lipid nanoparticles (CSLN) were developed and physicochemically analyzed. The ingredients and methods adopted in this study promoted the successful preparation of CSLN with a monodispersed particle size of 218.4–238.6 nm and a polydispersity index of 0.156-0.350. A differential scanning calorimetric assay demonstrated that CUM was incorporated. The atomic force microscopy images showed uniform spherical particles, and light scattering technique confirmed the size of the particles. The zeta potential of the CSLN was +23.1 to +30.1 mV, which is important in targeting the drug to the diseased tissue that presents unregulated apoptosis. All formulations behaved as controlled drug delivery systems of CUM, as demonstrated by an *in vitro* drug release study, which delayed the start of drug release from formulations. At the end of the experiment, the formulations had released 14.74-21.23% of the incorporated CUM. In conclusion, the results suggest the potential of this CSLN as a controlled CUM delivery system for the treatment of SD.

1. Introduction

Skin disorders such as skin cancer and autoimmune disorders such as psoriasis can lead to a deregulation of apoptosis. Apoptosis is a phenomenon highly regulated by complex pathways and promoter or inhibitor mechanisms. Deregulation of this process results in the disruption of homeostasis in tissues, resulting in pathological conditions. One regulatory mechanism of apoptosis is the increased phosphatidylserine (a negatively charged molecule) expression in the outer layer of the membrane of cells. This leaves the diseased tissue with a higher negative charge density to facilitate recognition by immune cells, which are responsible for removing the diseased tissue (Lima et al. 2009; Riedl et al. 2011, 2015; Li et al. 2016).

Furthermore, skin diseases, such as cancer, and autoimmune disorders are difficult to treat; patients usually show resistance to conventional therapies and often show severe side effects (Leboit et al. 2006; Petch et al. 2012; Oliveira et al. 2014; Mýsliwiec et al. 2016).

A wide variety of plants, particularly those with flavonoids or phenolic substances in their composition, such as quercetin, resveratrol, and curcumin (CUM), present chemopreventive properties resulting from their antioxidant and anti-inflammatory abilities (Fujimura et al. 2016). Laboratory and epidemiological studies have shown that routine intake of polyphenolic compounds can provide some protection against skin disorders such as melanoma (Mazzarino et al. 2011).

Regardless of potential use of CUM in the prevention and treatment of skin disorders, its clinical applications has been limited due to its physicochemical properties. For example, CUM has low water solubility in acidic and physiological pH conditions, rapid hydrolysis at an alkaline pH, and is unstable when exposed to light, making it difficult for its incorporation and preservation into conventional pharmaceutical forms (Sharma et al. 2005; Chen et al. 2012; Lestari and Indrayanto 2014). Furthermore, CUM has poor oral bioavailability; therefore, dermal administration can be a convenient alternative to target it to the site of action. Thus, technological strategies that have the ability to efficiently compartmentalize several groups of active ingredients, as well as modify their properties and behavior in biological environments, are promising for the administration of such substances (Mainardes et al. 2006; Souza et al. 2012; Gonçalez et al. 2013; Santos et al. 2013; Gonçalez et al. 2015; Soni and Yadav 2016; Gong and Chen 2016). Solid lipid nanoparticles (SLN) are gaining prominence as a drug delivery system owing to their ability to solubilize lipophilic active ingredients, increase physical and chemical stability of labile molecules, control release for drug delivery, lower skin irritation, and reduce particle size (Mei et al. 2003; Guterres et al. 2007; Liu et al. 2007; Marcato 2009). The small size presented by these systems can increase their contact with the stratum corneum, thus increasing their accumulation at this region, which may favor the controlled release of the drug. The composition of the SLN matrix allows for the exchange of lipids between the outer layers of the skin, which could increase the permeation of the drug by allowing its passage into the deeper skin layers, where diseases are located (Taveira et al. 2011; Rigon et al. 2015).

CUM-loaded cationic SLN (CUM-loaded CSLN) can directly promote targeted drug delivery to diseased tissue, thus reducing adverse effects on normal cells. Consequently, the positive charge provided by these formulations may promote drug targeting to cells in a deregulated apoptosis process that has a high-density negative charge due to exposure to phosphatidylserine on the surface of cell membranes. Therefore, the present study aimed to develop CUM-loaded CSLN to enhance the use of CUM in a topical treatment for skin disorders (Iwasaki et al. 2009; Sakamoto et al. 2010).

2. Investigations, results and discussion

2.1. Development of CSLN

For the development of CSLN, SA was used as the lipid phase, which is a fairly pure lipid, along with C888, which is a complex of

glycerides made of large carbon chains with a more heterogeneous composition, or each was used alone. The aim was to see how the drug interacted with these different composition formulations.

The concentration of P407 used was above the critical micelle concentration of the 10^{-4} M reported by Lee et al. (2003). This enabled monomers of P407 to organize into spherical micelles and form a film on the surface of the CSLN giving increased physical stability to the system through steric arrangement. It has been reported that the use of more than one surfactant contributes to the stability of a formulation (Karolewicz 2016). The addition of CB gives a positive charge to CSLN and promotes repulsion between the particles. This further reduces the probability of an agglomeration and increases the viscosity of the medium in which such particles are dispersed, assuring a long period of stability for the product (Severino et al. 2011).

A low concentration (0.025%) of CUM was incorporated into the developed CSLN because this formulation is composed of a chain of saturated lipids, which form a highly organized compact lipid core with little space for drug incorporation (Marcato 2009).

2.2. Evaluation of stability of CUM-unloaded and CUM-loaded CSLN

The formulations were prepared with different lipid phases, CSLN-1 composed of SA, CSLN-3 of C888 and CSLN-2 of a mixture of the two.

The stability of the formulations was assessed for 90 days and the results relating to CSLN-1, CSLN-2, and CSLN-3 are presented in Tables 1, 2, and 3, respectively, with and without CUM.

Table 1 shows that CUM-unloaded CSLN-1 showed a significant increase in Dnm with increased storage time. With the incorporation of CUM, the behavior was the same and indicated particle aggregation over time, thus forming larger structures (Jiang et al. 2009). During the study period, CUM-unloaded CSLN-1 showed an average Dnm of 225-415 nm and CUM-loaded CSLN-1, an average of 240-390 nm. There was a small increase in the PdI value of the formulations prepared with SA. CUM-unloaded CSLN-1 showed an average PdI of 0.156-0.212 and CUM-loaded CSLN-1, an average of 0.183-0.232, both with a relatively homogeneous size distribution (Table 1).

The zeta potential (ZP) is generated when an electrically charged particle is dispersed through a medium and results in the formation of an electric potential between the particle surface and the medium. This reaction results in changes on the particle surface to attract counter ions (Thielbeer et al. 2011). Throughout the storage period, CUM-unloaded CSLN-1 and CUM-loaded CSLN-1 showed an average ZP of +29 to +32 mV (Table 1), relative to the minimum ZP required for good physical stability of a system (Freitas and Müller 1998).

Table 2 shows that formulations prepared with a mixture of lipids had a significant increase in Dnm with storage time due to an aggregation of the particles. During the storage period, CUM-unloaded CSLN-2 showed an average Dnm of 228-331 nm and CUM-loaded CSLN-2, an average between 237-316 nm. The CUM-unloaded and CUM-loaded CSLN-2, initially, showed low PdI values (Table 2). However, they exhibited a significant increase over time, suggesting heterogeneity in the distribution of Dnm, which may be related to the two lipids with very different chemical structures

Table 1: Stability of curcumin-unloaded cationic solid lipid nanoparticles (CUM-unloaded CSLN)-1 and CUM-loaded CSLN-1 over 90 days

	CUM-unloaded CSLN-1			CUM-loaded CSLN-1		
Time (days)	Dnm (nm)	PdI	ZP (mV)	Dnm (nm)	PdI	ZP (mV)
1	224.97±4.15^{a}	0.156±0.009^{a}	29.45±0.97^{a}	238.57±7.22^{a}	0.185±0.021^{a}	30.08±0.64^{a}
7	261.42±12.68^{b}	0.196±0.023^{b}	30.32±0.64^{a,b}	286.03±11.73^{b}	0.192±0.013^{a}	30.88±0.50^{a,b}
15	301.39±13.04^{c}	0.196±0.028^{b}	31.19±0.70^{b,c}	315.15±10.77^{c}	0.183±0.022^{a}	30.60±0.89^{a,b}
30	341.28±10.93^{d}	0.190±0.023^{b}	31.25±0.55^{b,c}	347.43±10.06^{d}	0.197±0.024^{a,b}	31.64±1.05^{b}
60	376.23±9.82^{e}	0.194±0.012^{b}	30.72±1.24^{b}	385.74±24.67^{e}	0.232±0.052^{b}	30.61±1.35^{a,b}
90	415.29±13.30^{f}	0.212±0.013^{b}	32.72±0.78^{c}	394.34±16.77^{e}	0.208±0.035^{a,b}	29.84±0.71^{a}

*Means (mean ± standard deviation) followed by the same letter in the column are not significantly different from each other, as verified using Tukey's test, α = 5%.

Table 2: Stability of curcumin-unloaded cationic solid lipid nanoparticles (CUM-unloaded CSLN)-2 and CUM-loaded CSLN-2 over 90 days

	CUM-unloaded CSLN-2			CUM-loaded CSLN-2		
Time (days)	Dnm (nm)	PdI	ZP (mV)	Dnm (nm)	PdI	ZP (mV)
1	228.19±5.17^{a}	0.265±0.029^{a}	27.28±0.81^{a}	237.11±6.40^{a}	0.318±0.034^{a}	26.99±2.21^{a}
7	276.22±7.21^{b}	0.423±0.034^{b}	30.88±0.97^{b}	306.11±19.04^{b}	0.571±0.066^{b}	31.10±1.24^{b}
15	303.54±8.41^{c}	0.576±0.088^{c}	30.89±1.36^{b}	303.93±11.09^{b}	0.579±0.088^{b}	31.00±0.91^{b}
30	318.38±20.47^{c,d}	0.656±0.028^{d}	31.03±1.09^{b}	308.23±13.22^{b}	0.631±0.036^{b,c}	31.03±2.09^{b}
60	325.21±19.07^{d}	0.678±0.039^{d}	29.80±1.26^{b}	312.57±18.58^{b}	0.656±0.034^{c}	30.05±1.62^{b}
90	331.24±22.76^{d}	0.692±0.047^{d}	29.68±1.45^{b}	316.75±19.73^{b}	0.688±0.034^{c}	29.12±1.25^{b}

*Means (mean ± standard deviation) followed by the same letter in the column are not significantly different from each other, as verified using Tukey's test, α = 5%.

Table 3: Stability of curcumin-unloaded cationic solid lipid nanoparticles (CUM-unloaded CSLN)-3 and CUM-loadedCSLN-3 over 90 days

	CUM-unloaded CSLN-3			CUM-loaded CSLN-3		
Time (days)	Dnm (nm)	PdI	ZP (mV)	Dnm (nm)	PdI	ZP (mV)
1	219.09±12.25^{a}	0.340±0.039^{a}	23.11±1.72^{a}	218.44±11.43^{a}	0.350±0.045^{a}	25.58±1.10^{a}
7	235.60±4.65^{b,c}	0.387±0.013^{b}	24.89±1.16^{b}	239.04±22.37^{b,c}	0.345±0.044^{a}	25.63±0.88^{a}
15	233.80±13.18^{b,c}	0.348±0.046^{a,b}	24.62±0.81^{b}	250.93±10.99^{b}	0.382±0.024^{a,b}	25.88±1.24^{a}
30	225.59±14.35^{a,c}	0.364±0.024^{a,b}	24.59±0.45^{b}	232.94±18.33^{a,c}	0.352±0.036^{a}	23.83±0.90^{b}
60	236.57±13.41^{b,c}	0.455±0.054^{c}	22.33±1.33^{a}	247.72±27.67^{b,c}	0.403±0.026^{b}	20.62±1.59^{c}
90	230.75±12.22^{c}	0.383±0.013^{a,b}	22.57±0.83^{a}	235.69±16.74^{c}	0.404±0.018^{b}	22.54±0.84^{b}

*Means (mean ± standard deviation) followed by the same letter in the column are not significantly different from each other, as verified using Tukey's test, α = 5%.

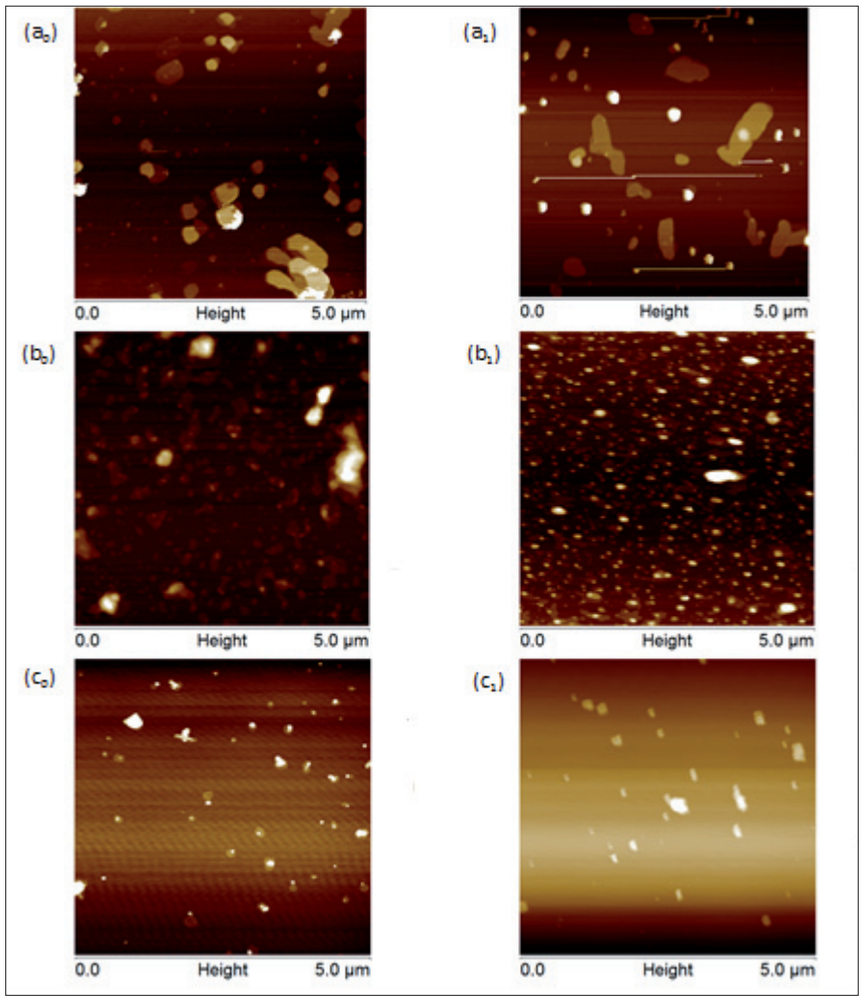

Fig. 1. Photomicrographs of (a) CSLN-1, (b) CSLN-2, and (c) CSLN-3 samples analyzed with AFM. Letters with a "0" refer to formulations without CUM and those with a "1" refer to formulations with CUM.

used to make the system (Krause et al. 2010). During the study, CUM-unloaded CSLN-2 showed an average PdI of 0.265-0.690 and CUM-loaded CSLN-2, an average of 0.318-0.690. CUM-unloaded and CUM-loaded CSLN-2 showed an average ZP of +27 to +31 mV (Table 2).

Table 3 shows that CSLN-3, with and without CUM, showed a significant increase in Dnm throughout the storage time; however, the variation was low during the entire study. The CUM-unloaded CSLN-3 showed an average Dnm of 200-240 nm and CUM-loaded CSLN-3, an average of 218-250 nm. The CUM-unloaded CSLN-3 showed a significant increase in the PdI throughout the storage time. The average PdI of this system was between 0.340 and 0.450. By incorporating CUM there was higher stability in the PdI values over time, showing a significant increase only after 60 days of storage. CUM-loaded CSLN-3 showed an average PdI of 0.340-0.400 during the 90 days.

When CUM-unloaded CSLN-3 and CUM-loaded CSLN-3 were produced, they presented high PdI values because of the C888 composition. C888 is a mixture of acylglycerides, with glyceryl tribehenate (28-32%), glyceryl dibehenate (52-54%), and glyceryl behenate (12-18%) as the main components, and behenic acid (>85%) as the main fatty acid, but other fatty acids (C16-C20) may also be present (Souto et al. 2006). The formation of the CSLN with these different lipids or different ratios of these lipids, with different Dnm, may have resulted in a greater PdI value in relation to the CSLN consisting of SA, which is a pure lipid (Severino et al. 2011). CUM-unloaded CSLN-3 had an average ZP of +22 to +25 mV and CUM-loaded CSLN-3, an average of +20 to +26 mV during the 90 days of storage (Table 3).

Finally, stability studies showed that CSLN-3 was the most stable, and displayed higher PdI values from the beginning, which indicates the formation of a more polydispersed system. However, CSLN-3 had the lowest variable average Dnm (Table 3), and was more stable than the other formulations.

2.3. Microscopic analysis

AFM was used to observe the morphological characteristics of CUM-unloaded CSLN and CUM-loaded CSLN. Figure 1 shows two-dimensional and three-dimensional photomicrographs of the formulations developed with and without the incorporation of CUM.

The drying process used to prepare the samples for microscopic analyses promoted an agglomeration of particles (Dubes et al. 2003), leaving a few isolated, which confirm that CSLN are round in shape with a particle size in the nanometer range (Fig. 1) (Zamarioli et al. 2015). The AFM images showed uniform spherical particles and confirmed the sizes determined by a dynamic light scattering technique.

2.4. Differential scanning calorimetry (DSC)

Figure 2 shows the DSC curves of the raw materials used to prepare the formulations, as analyzed separately. Figure 3 shows the DSC curves obtained from the analysis of CUM-unloaded CSLN, CUM-loaded CSLN, and CUM alone.

Table 4 describes the peak temperatures and enthalpies obtained from the DSC curves of the components used to prepare the formu-

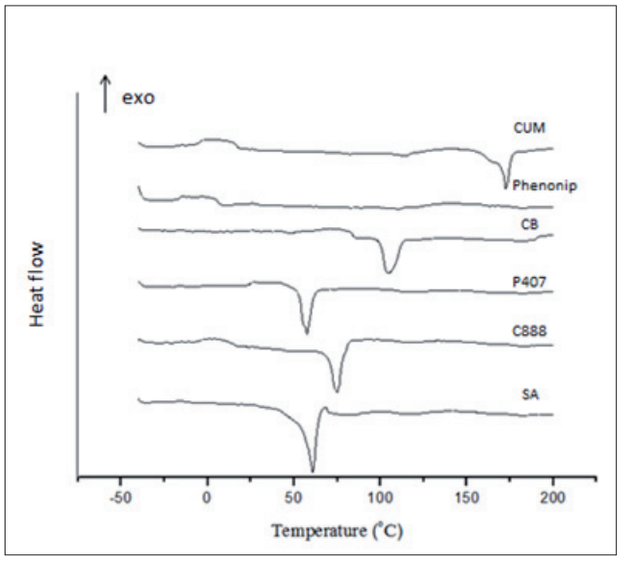

Fig. 2: Differential scanning colorimetry (DSC) curves of the raw materials used for the preparation of the CSLN as analyzed separately. Legend: SA: stearic acid; C888: Compritol 888 ATO; P407: poloxamer 407; CB: cetrimonium bromide; CUM: curcumin.

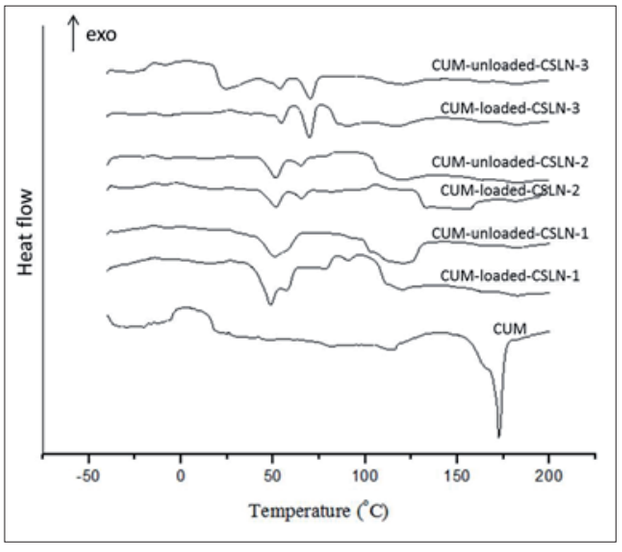

Fig. 3: Differential scanning colorimetry (DSC) curves obtained from the analysis of the formulations developed with and without the incorporation of CUM and of CUM alone. Legend: CUM: curcumin.

lations and CSLN with and without CUM. The expected enthalpy was calculated according to the composition of the CSLN.

In Fig. 2, the endothermic events indicate the melting of the components of the formulations, and Table 4 describes the melting point of the components, as analyzed individually. The components of the formulations presented structural modifications to produce the CSLN, observed by the decrease in melting point of the components, which was observed in all formulations, indicating the formation of the system (Table 4) (Vaghasiya et al. 2013). The DSC curves of all of the formulations had no endothermic event at the CB melting point region. This probably was because the component was used at a low concentration in the formulations and its fusion could not be observed (Fig. 3).

In analyzing each formulation, CUM-unloaded CSLN-1 showed a junction between the peaks relating to P407 and SA, with the obtained enthalpy lower than expected. This indicates that these components interacted in the system training. However, with the

Table 4: Expected and obtained enthalpy values from differential scanning colorimetry (DSC) testing of the components and of the cationic solid lipid nanoparticles (CSLN) formulations, with and without the incorporation of CUM

Samples	T_{peak} (°C)	$\Delta H_{expected}$	$\Delta H_{obtained}$
SA	61.0	-	203.0
C888	75.0	-	182.8
P407	57.5	-	131.6
CB	105.0	-	153.1
CUM	172.5	-	138.1
CUM-unloaded CSLN-1	48.8 / 58.0	161.4	147.7
CUM-loaded CSLN-1	50.0 / 57.0	160.9	163.8
CUM-unloaded CSLN-2	51.0 / 65.0	104.3 / 51.3	61.0 / 21.0
CUM-loaded CSLN-2	51.0 / 65.0	104.0 / 51.2	67.8 / 16.9
CUM-unloaded CSLN-3	55.0 / 70.0	47.3 / 102.7	23.1 / 73.6
CUM-loaded CSLN-3	54.0 / 71.0	47.2 / 102.4	42.4 / 77.4

incorporation of CUM, the obtained enthalpy increased. There was also no observed endothermic event at the CUM melting point region, indicating that CUM interacted with the components of the formulation (Fig. 3 and Table 4). In the CUM-unloaded and CUM-loaded CSLN-2, a junction between the peaks relating to P407 and SA and an endothermic event related to C888 were individually set, therefore Table 4 shows two expected and obtained enthalpies. There was a reduction in the enthalpies obtained in relation to what was expected, indicating the interaction of these compounds in the system training. The incorporation of CUM also led to an increased obtained enthalpy related to P407 and SA components, indicating that CUM interacted with the formulation components (Fig. 3 and Table 4) (Vaghasiya et al. 2013).

In the DSC curves of CUM-unloaded and CUM-loaded CSLN-3, two completely separate endothermic events were observed (Fig. 3), related to P407 and C888. Therefore, Table 4 shows two obtained and expected enthalpies relating to each of these compounds. These two formulations where the enthalpy obtained was lower than expected indicate that the compounds were in an amorphous arrangement while forming the system (Table 4). Moreover, in comparing the obtained enthalpies for CUM-unloaded and CUM-loaded CSLN-3, an increase can be seen in relation to these two components, indicating that the CUM was solubilized in both C888 and P407.

2.5. "In vitro" drug release study for CUM-loaded CSLN

The HPLC method using for quantification of drug release of CUM from CUM-loaded CSLN showed an excellent linearity ($r = 0.9993$), it was obtained with regression equations of $y = 0.1642x - 0.0145$, the detection limit was of 0.0039 µg/mL, the quantitation limit of 0.0129 µg/mL. In addition, the validated method presented accuracy with satisfactory recovery, and repeatability intermediate precision and reproducibility with percentage relative standard deviation (RSD) within the standards established by International Conference on Harmonisation (2005) (Branch 2005).

Figure 4 shows the CUM release profiles from the CUM-loaded CSLN-1, CSLN-2, and CSLN-3 and CUM solution. After 1 h, 27.50% of CUM could be measured from the CUM solution and after 20 h, 40.47% of CUM was present. Whereas, from the developed CUM-loaded CSLN, the release of CUM started after 16 h of contact with the synthetic membrane. After 20 h, only 21.23±1.27% of CUM was released from CUM-loaded CSLN-1, 15.80±0.95% of CUM from CUM-loaded CSLN-2, and 14.75±7.35% of CUM from CUM-loaded CSLN-3. After 20 h, the percentage of CUM released from the CUM solution was significantly higher than that of the CUM-loaded CSLN formulations ($p < 0.01$). There were no significant differences between the developed formulations ($p > 0.05$).

The system with C888, as a lipid phase, showed high variability in the dissolution profiles of CUM. This may result from the inho-

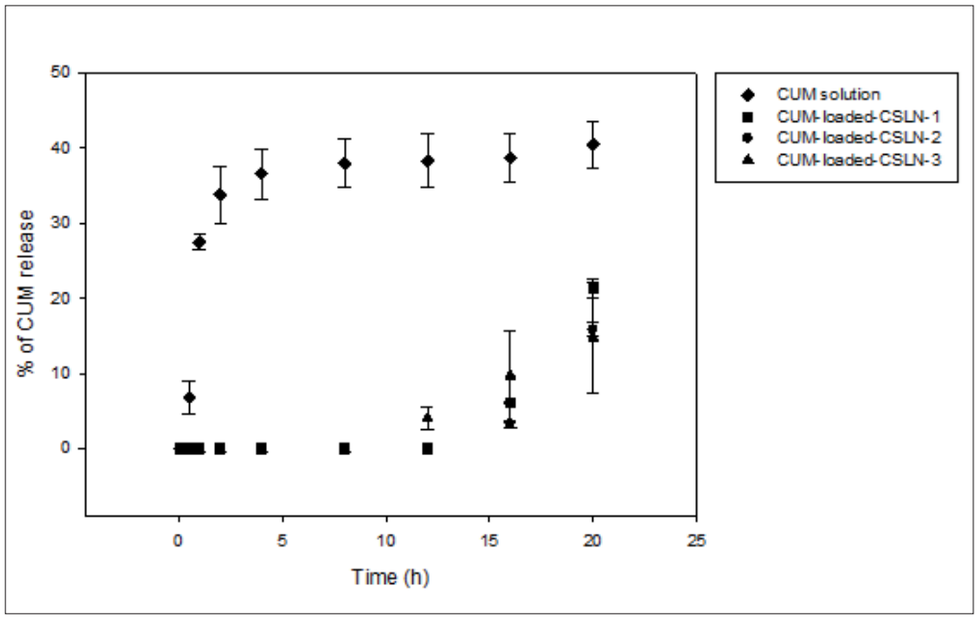

Figure 4. CUM release profiles

mogeneous arrangement of C888 for nanoparticle formation. In contrast, SA has a smaller chemical structure and better molecular interaction. Consequently, the system made with SA presented a lower variability in dissolution profile of CUM.

Mathematical models can be used in formulation optimization, helping to select and prepare a formulation with the determined release characteristics. These models generate a general equation that reflects the dissolution curve and drug release as a function of parameters related to the pharmaceutical form. For example, a comparison is possible of drug release profiles for formulations manufactured with different excipients (Costa et al. 2002; Peppas and Narasimhand 2014).

The developed formulations were adjusted using the Weibull model and exhibited a sigmoidal curve ($b > 1$) of the CUM release profile from the formulations. This indicates that a complex mechanism governs the release process (Table 5) (Papadopoulou et al. 2006). The drug released from the nanoparticles was slow up until the inflection point, corresponding to periods of system destructuration, and after that, the CUM release increased gradually for up to 20 hours (Fig. 4).

Based on the results in Table 5, CUM solution samples fit well to the Weibull model; however, they exhibited another release pathway corresponding to a parabolic curve ($b < 1$). There was no resistance of CUM passage to the receiver compartment. It showed a quick increase of measured CUM in the receptor solution, which reached a plateau after 4 h (Fig. 4).

2.6. Conclusions

Nanoparticles were obtained with positive ZP values and a Dnm of about 200 nm. The CUM-unloaded CSLN-3 proved to be the most stable formulation and did not show significant Dnm or PdI alterations after the incorporation of CUM. AFM images confirmed the results obtained with the photon correlation technique that the developed formulations are dispersions of spherical particles with sizes in the nanometer range. The DSC assay showed that the components of the formulations interacted as a training system and the formulations with CUM presented an obtained enthalpy, related to the lipids and P407, higher than the expected enthalpy. This indicates that CUM interacted with compounds and, therefore, was incorporated into the formulations. After 20 h of an *in vitro* drug release study, the percentage of CUM measured in the receptor compartment from the CUM solution was significantly higher than that of the formulations ($p < 0.01$), and there was no significant difference between the developed formulations ($p > 0.05$). Furthermore, the developed formulations showed a release profile of CUM adjusted to the Weibull model. Thus, the CUM-loaded CSLN developed in this work presented a controlled CUM delivery system and has promising characteristics to become an interesting platform for skin disorder treatments, although, further biological studies are needed to confirm this theory.

3. Experimental

3.1. Materials

All chemicals were obtained commercially. Stearic acid (SA) was purchased from Via Farma (São Paulo, Brazil), compritol 888 ATO (C888) from Gattefossé (Cedex, France), cetrimonium bromide (CB) from Vetec (Rio de Janeiro, Brazil), poloxamer 407 (P407) and curcumin (CUM), with 77% purity, from Sigma-Aldrich (St. Louis, MO, USA), and Phenonip® from Fagron (São Paulo, Brazil). Methanol, acetonitrile, and absolute ethanol, all HPLC grade, were purchased from J.T.Baker (Center Valley, PA, USA), glacial acetic acid from Quemis (Joinville, Brazil), polysorbate 80 and propylene glycol from Synth (Diadema, SP, Brazil) and synthetic hydrophilic polysulfone membranes (HT Tuffryn®) from PALL Corporation (Port Washington, NY, USA). The water used was ultrapure (Milli-Q; Millipore Inc., USA).

3.2. Development of CSLN

CSLN were prepared employing a method adapted from Castelli et al. (2005). To prepare the pre-emulsion, the lipid phase, composed of SA, C888, or a mixture of

Table 5: *In vitro* curcumin (CUM) release coefficient, obtained by different mathematical models for CUM-loaded cationic solid lipid nanoparticles (CSLN)-1, CSLN-2, and CSLN-3 and CUM solution

Mathematical models	R squared value (R2)			
	CUM Solution	CUM-loaded CSLN-1	CUM-loaded CSLN-2	CUM-loaded CSLN-3
Korsmeyer-Peppas	0.7549	0.9418	0.9683	0.9732
Higuchi	0.4660	0.4689	0.4279	0.6281
First Order Kinetics	-0.1804	0.6795	0.6367	0.8520
Weibull	**0.9987**	**1.0000**	**1.0000**	**0.9999**
Zero Order Kinetics	0.4549	0.7567	0.7139	0.9063

Table 6: Composition of cationic solid lipid nanoparticles (CSLN) developed

Formulation	SA (%)	C888 (%)	P407 (%)	CB (%)	Phenonip® (%)
CUM-unloaded CSLN-1	5	0	3.2	0.7	0.75
CUM-unloaded CSLN-2	2.5	2.5	3.2	0.7	0.75
CUM-unloaded CSLN-3	0	5	3.2	0.7	0.75

*CUM-loaded CSLN contained 0.025% of CUM.

the two, was heated about 5-10 °C above its melting point, and was dispersed in an aqueous solution containing a mixture of surfactants, P407 and CB, heated to the same temperature, and the pre-emulsion was stirred using a magnetic stirrer for 30 s while maintaining the temperature (model 752A, Fisatom, São Paulo, Brazil). The resulting pre-emulsion was sonicated for 20 min at 12-17 W (Q700 Ultrasonic processor, Qsonica, Newton, CT, USA), and the samples were placed in an ice bath.
For the preparation of the CUM-loaded CSLN, 0.025% of CUM was added to the melted lipid phase during the preparation of the pre-emulsion. They were prepared with 40 mL of the aqueous dispersion of nanoparticles with a subsequent addition of 300 µL of the preservative, phenonip® (phenoxyethanol + parabens) (Wu et al. 2009; Obeidat et al. 2010; Hung et al. 2011; Ngan et al. 2014). To eliminate the titanium that can be given off during the sonication process, the formulations were centrifuged at 1,000 x g for 10 minutes (Spectrafuge™ 16 M Microcentrifuge, Labnet, USA) (Agayan et al. 2004). The compositions of the formulations developed in this study are presented in Table 6.

3.3. Determination of average hydrodynamic diameter

The average hydrodynamic diameter (Dnm) and polydispersivity index (PdI) were determined by photon correlation spectroscopy using a Zetasizer Nano NS (Malvern Instruments, Malvern, UK). These measurements were performed at 25 °C using ultrapure water as the dispersing medium and a dilution of the suspensions of CSLN at a ratio of 1:100, and the results were analyzed using *Zetasizer software, version 7.10*.

3.4. Zeta potential analysis

Zeta Potential (ZP) was analyzed by determining the particle electrophoretic mobility using a Zetasizer Nano NS. The CSLN suspensions were diluted in ultrapure water at a ratio of 1:100 and measured at 25 °C then analyzed with *Zetasizer software, version 7.10*.

3.5. Evaluation of stability of CUM-unloaded and CUM-loaded CSLN

For the stability test, three samples of each formulation were considered (Table 6), with and without the incorporation of CUM, which were then stored in amber glass container at 5 °C for 90 days. Dnm, PdI, and ZP were determined for each sample, in triplicate, 24 h after its preparation and after being stored for 7, 15, 30, 60, and 90 days. The stability data were evaluated using the mean ± standard deviation from an analysis of variance (ANOVA) statistical test for repeated measurements with a significance level of 5%, using *Statistica software, version 7*.

3.6. Microscopic analysis

The morphology of CSLN was determined using atomic force microscopy (AFM). A drop of the sample was placed on a mica plate, which was centrifuged in a spin coater for 30 s at 500 rpm and 1 min at 5000 rpm (model KW-4A, Spin Coater Centrifuge – SPI Supplies, USA). The mica plate was observed under a scanning microscope (Dimension Icon, Bruker, Germany) and processed using *Nanoscope software, version 1.40*.

3.7. Differential scanning calorimetry (DSC)

Measurements were carried out using a differential scanning calorimeter (Q10 Model, TA Instruments, New Castle, DE, USA). DSC curves were obtained under the following conditions: sample mass of about 5 mg, measured in an aluminum crucible at temperature range from -40 to 200 °C (10 °C/min) under a nitrogen dynamic atmosphere. The raw materials used in the preparation of the formulations and lyophilized formulations, without cryoprotectants, were measured. Conventionally, it was adopted as exothermic peaks, those pointed upward. The results were plotted using *Origin software, version 8* (OriginLab Corporation) and analyzed with *TA Instruments Universal Analysis software*.

3.8. "In vitro" drug release study for CUM-loaded CSLN

The *in vitro* assay for CUM release from CUM-loaded CSLN was performed using a synthetic hydrophilic polysulfone membrane (HT Tuffryn®) with a 0.45 µm pore size and 25 mm diameter. The receptor solution consisted of 0.2 M potassium phosphate buffer (pH 7.4) with 1% polysorbate 80 (v/v), 15% propylene glycol (1,2-propanediol) (v/v), and 5% absolute ethanol (HPLC grade (v/v)) to create a perfect sink condition, since CUM has limited solubility in buffer (Koop et al. 2015). Samples (300 µL) of formulations or CUM solution (250 µg/mL), made with a receptor solution, were transferred to the donor compartment of a Franz diffusion cell (1.77 cm^2 area of exposure). Then, 3 mL of the receptor solution was collected at 5 and 30 min, 1, 2, 4, 8, 12, 16, 20, and 24 h during the experiment. The same volume of fresh receptor solution was then replaced.
The amount of drug released was determined by HPLC, considering the dilution of each sample, using a method validated by Fonseca-Santos et al. (2016). The method employs Varian HPLC-equipment with a ProStar® spectrophotometric detector, 330-UV-VIS-PDA, and Rheodine-VC-125, an autosampler ProStar® Varian (model 410), and automatic injection of 20 µL. A C18 column, 250 mm × 4.6 mm, with a 5 µm particle size was used. The mobile phase was a 50:50 mixture of acetonitrile:acidic water (2 % acetic acid) with a flow of 1.2 mL/min at 33 °C and a CUM retention time of 12 min.
An ANOVA was used to search for significant differences in the mean percentage of CUM released from different CUM-loaded CSLN after 24 h. This analysis was performed using *Statistica software, version 7*. The results were evaluated for the mathematical model that best explained the drug release process of the formulations developed using *SigmaPlot software, version 10.0*. The model associated with the highest R^2 value was determined to be the best to represent the behavior of drug release process of the formulations.

Acknowledgments: This work was financially supported by Fundação de Amparo à Pesquisa do Estado de São Paulo (FAPESP), Conselho Nacional de Desenvolvimento Científico e Tecnológico (CNPq), and Programa de Apoio ao Desenvolvimento Científico (PADC-UNESP).

Conflicts of interest: None declared.

References

Agayan, RR, Horvath T, McNaughton BH, Anker JN, Kopelman R (2004) Optical manipulation of metal-silica hybrid nanoparticles. Proceedings of SPIE 5514: 502-513.

Branch SK (2005) Guidelines from the international conference on harmonisation (ICH). J Pharm Biomed Anal 38: 798-805.

Castelli F, Astelli F, Puglia C, Sarpietro MG, Rizza L, Bonina F (2005) Characterization of indomethacin-loaded lipid nanoparticles by differential scanning calorimetry. Int J Pharm 304: 231–238.

Chen, Y; Wu, O; Zhang, Z; Yuan, L; Liu, X; Zhou, L (2012) Preparation of curcumin-loaded liposomes and evaluation of their skin permeation and pharmacodynamics. Molecules 17: 5972-5987.

Costa PJC (2002) Avaliação in vitro da lioequivalência de formulações farmacêuticas. Rev Brasil Ciênc Farm 38: 141-153.

Dubes A, Parrot-Lopez H, Abdelwahed W, Degobert G; Fessi H, Shahgaldian P, Coleman AW (2003) Scanning electron microscopy and atomic force microscopy imaging of solid lipid nanoparticles derived from amphiphilic cyclodextrins. Eur J Pharm Biopharm 55: 279-282.

Fonseca-Santos B, Gremiao MPD, Chorilli M (2016) A simple reversed phase high-performance liquid chromatography (HPLC) method for determination of in situ gelling curcumin-loaded liquid crystals in in vitro performance tests. Arabian J Chem https://doi.org/10.1016/j.arabjc.2016.01.014

Freitas C, Müller RH (1998) Effect of light and temperature on zeta potential and physical stability in solid lipid nanoparticle (SLN™) dispersions. Int J Pharm 168: 221–229.

Fujimara AT, Martinez RM, Pinho-Ribeiro FA, Lopes Dias da Silva AM, Baracat MM, Georgetti SR, Verri WA, Chorilli M, Casagrande R (2016) Resveratrol-loaded liquid-crystalline system inhibits UVB-induced skin inflammation and oxidative stress in mice. J Nat Prod 79: 1329-1338.

Gonçalez ML; Corrêa MA; Chorilli M (2013) Skin delivery of kojic acid-loaded nanotechnology-based drug delivery systems for the treatment of skin aging. BioMed Res Int 2013: 1-9.

Gonçalez ML, Marcussi DG, Calixto GMF, Corrêa MA, Chorilli M (2015) Structural characterization and in vitro antioxidant activity of kojic dipalmitate loaded W/O/W multiple emulsions intended for skin disorders. BioMed Res Int 2015: 1-8.

Gong R, Chen G (2016) Preparation and application of functionalized nano drug carriers. Saudi Pharm J 24: 254–257.

Guterres SS, Alves MP, Pohlmann AR (2007) Polymeric nanoparticles, nanospheres and nanocapsules, for cutaneous application. Drug Target Insights 2: 147-157.

Hung LC, Basri M, Tejo BA, ismail R, Nang HL, Abu Hassan H, May CY (2011) An improved method for the preparations of nanostructured lipid carriers containing heat-sensitive bioactives. Colloids and Surfaces B: Biointerfaces 87: 180-186.

Iwasaki T, Ishibashi J, Tanaka H, Sato M, Asaoka A, Taylor D, Yamakawa M (2009) Selective cancer cell cytotoxicity of enantiomeric 9-mer peptides derived from beetle defensins depends on negatively charged phosphatidylserine on the cell surface. Peptides 30: 60–668.

Jiang J, Oberdörster G, Biswas P (2009) Characterization of size, surface charge, and agglomeration state of nanoparticle dispersions for toxicological studies. J Nanopart Res 11: 77–89.

Karolewicz B (2016) A review of polymers as multifunctional excipients in drug dosage form technology. Saudi Pharm J 24: 525–536.
Koop HS, Freitas RA, Souza MM, Savi jr. R, Silveira JLM (2015) Topical curcumin-loaded hydrogels obtained using galactomannanfrom Schizolobium parahybae and xanthan. Carbohydr Polym 116: 229–236.
Krause B, Mende M, Pötschke P, Petzold G (2010) Dispersability and particle size distribution of CNTs in an aqueous surfactant dispersion as a function of ultrasonic treatment time. Carbon 48: 2746–2754.
Leboit PE, Burg G, Weedon D, Sarasin A (eds) (2006) World Health Organization Classification of Tumours. Pathology and Genetics of Skin Tumours, 1st ed., IARC Press: Lyon, pp. 48-119.
Lee K, Shin SC, Oh I (2003) Fluorescence spectroscopy studies on micellization of Poloxamer 407 solution. Arch Pharm Res 26: 653-658.
Lestari MLAD, Indrayanto G (2014) Curcumin. Profiles of Drug Substances, Excipients, and Related Methodology 39: 113-204.
Li, K, Zhou, R, Jia, WW, Li Z; Li J; Zhang P, Xiso T (2016) Zanthoxylum bungeanum essential oil induces apoptosis of HaCaT human keratinocytes. J Ethnopharmacol 186: 351–361.
Lima LG, Chammas R, Monteiro RQ, Moreira MEC, Barcinski MA (2009) Tumor-derived microvesicles modulate the establishment of metastatic melanoma in a phosphatidylserine-dependent manner. Cancer Letter 283: 168–175.
Liu J, Hu W, Chen H, Ni Q, Xu H, Yang X (2007) Isotretinoin-loaded solid lipid nanoparticles with skin targeting for topical delivery. Int J Pharm 328: 191-195.
Mainardes RM, Urban MCC, Cinto PO, Chaud MV, Evangelista RC, Gremião MPD (2006) Liposomes and micro/nanoparticles as colloidal carriers for nasal drug delivery. Curr Drug Deliv 3: 275-285.
Marcato PD (2009) Preparação, caracterização e aplicações em fármacos e cosméticos de nanopartículas lipídicas sólidas. Revista eletrônica de farmácia 6: 1-37.
Mazzarino L, Silva LFC, Curta JC, Licinio MA, Costa A, Leticia K, Pacheco LK, Siqueira JM, Montanari J, Romero E, Assreury J, Santos-Silva MC. Lemos-Senna E (2011) Curcumin-loaded lipid and polymeric nanocapsules stabilized by nonionic surfactants: an *in vitro* and *in vivo* antitumor activity on B16-F10 melanoma and macrophage uptake comparative study. J Biomed Nanotechnol 7: 406–414.
Mei Z, Chen H, Weng T, Yang Y, Yang X (2003) Solid lipid nanoparticle and microemulsion for topical delivery of triptolide. Eur J Pharm Biopharm 56: 189-196.
Mysliwiec H, Mysliwies P, Baran A, Flisiak W (2016) Dithranol treatment of plaque-type psoriasis increases serum TNF-like weak inducer of apoptosis (TWEAK). Adv Med Sci 61: 207–211.
Ngan CL, Basri M, Lye FF, Fard Msaoumi HR, Tripathy M, Karjiban RA, Abdul-Malek E (2014) Comparison of process parameter optimization using different designs in nanoemulsion-based formulation for transdermal delivery of fullerene. International J Nanomed 9: 4375-4386.
Oliveira C, Lourenco GJ, Rinck-Junioe JA, Cintra ML, Moraes AM, Lima CSP (2014) Association between genetic polymorphisms in apoptosis-related genes and risk of cutaneous melanoma in women and men. J Dermatol Sci 74: 135–141.
Obeidat WM, Schwabe K, Müller RH, Keck CM (2010) Preservation of nanostructured lipid carriers (NLC). Eur J Pharm Biopharm 76: 1: 56-67.
Papadopoulou V, Kosmidis K, Vlachou M, Macheras P (2006) On the use of the Weibull function for the discernment of drug release mechanisms. Int J Pharm 309: 44–50.
Peppas NA, Narasimhand B (2014) Mathematical models in drug delivery: How modeling has shaped the way we design new drug delivery systems. J Control Release 190: 75–81.
Petch D, Anderson RJ, Cunningham A, George SE, Hibbs DE, Liu R, Mackay SP, Paul A, Small DAP, Groundwater PW (2012) Design and synthesis of EGFR dimerization inhibitors and evaluation of their potential in the treatment of psoriasis. Bioorg med Chem 20: 5901–5914.
Riedl S, Rinner B, Asslaber M, Schaider H, Walzer S, Novak A, Lohner K, Zweytick D (2011) In search of a novel target — phosphatidylserine exposed by non-apoptotic tumor cells and metastases of malignancies with poor treatment efficacy. Biochim Biophys Acta 1808: 2638–2645.
Riedl S, Leber R, Rinner B, Schaider H, Lohner K, Zweytick D (2015) Human lactoferricin derived di-peptides deploying loop structures induce apoptosis specifically in cancer cells through targeting membranous phosphatidylserine. Biochim Biophys Acta 1848: 2918–2931.
Rigon RB, Oyafuso MH, Fujimura AT, Goncalez ML, Do Prado AH, Gremiao MPD, Chorilli M (2015) Nanotechnology-based drug delivery systems for melanoma antitumoral therapy: a review. BioMed Res Int 2015: 1-22.
Santos FK, Oyafuso MH, Kiill CP, Gremião MPD, Chorilli M (2013) Nanotechnology-based drug delivery systems for treatment of hyperproliferative skin diseases - a review. Curr Nanosci 9: 159-167.
Sakamoto JH, Ven ALV, Godin B, Blanco E, Serda RE, Grattoni A, Ziemys A, Bouamrani A, Hu T, Ranganathan SI, Rosa E, Martinez JO, Smid CA, Buchanan RM, Lee SY, Srinivasan S, Landry M, Meyn A, Tasciotti E, Liu X, Decuzzi P, Perrari M (2010) Enabling individualized therapy through nanotechnology. Pharmacol Res 62: 57–89.
Severino P, Pinho SC, Souto EB, Santana MHA (2011) Polymorphism, crystallinity and hydrophilic–lipophilic balance of stearic acid and stearic acid–capric/caprylic triglyceride matrices for production of stable nanoparticles. Colloids Surfaces B: Biointerfaces 86; 125–130.
Sharma RA, Gescher AJ, Steward WP (2005) Curcumin: the story so far. Eur J Cancer 41: 1955–1968.
Soni G, Yadav KS (2016) Nanogels as potential nanomedicine carrier for treatment of cancer: A mini review of the state of the art. Saudi Pharm J 24: 133–139.
Souto EB, Mehnert W, Müller RH (2006) Polymorphic behaviour of Compritol888 ATO as bulk lipid and as SLN and NLC. J Microencapsul 23: 4: 417–433.
Souza ALR, Kiill CP, Santos FK, Luz GM, Silva HR, Chorilli M, Gremião MPD (2012) Nanotechnology-based drug delivery systems for dermatomycosis rreatment. Curr Nanosci 8: 512-519.
Taveira SF, Araújo LMC, Santana DCAS, Monizo A, Freitas LAP, Lopez RFV (2011) Development of cationic solid lipid nanoparticles with factorial design-based studies for topical administration of doxorubicin. J Biomed Nanotechnol 8: 1–10.
Thielbeer F, Donaldson K, Bradley M (2011) Zeta potential mediated reaction monitoring on nano and microparticles. Bioconjug Chem 22: 2: 144–150.
Vaghasiya H, Kumar A, Sawant K (2013) Development of solid lipid nanoparticles based controlled release system for topical delivery of terbinafine hydrochloride. Eur J Pharm Sci 49: 311–322.
Wu X, Biatry B, Cazeneuve C, Guy RH (2009) Drug delivery to the skin from sub-micron polymeric particle formulations: influence of particle size and polymer hydrophobicity. Pharm Res 26: 1995-2001.
Zamarioli CA, Martins RM, Carvalho EC, Freitas LAP (2015) Nanoparticles containing curcuminoids (Curcuma longa): development of topical delivery formulation. Rev Brasil Farmacogn 25: 53–60.